

9th International Conference on Sustainability in Energy and Buildings, SEB-17, 5-7 July 2017,
Chania, Crete, Greece

Variations of PV module parameters with irradiance and temperature

Haider Ibrahim, Nader Anani

*Department of Engineering and Design, University of Chichester, Bognor Regis, PO21 1HR, UK.
n.anani@chi.ac.uk*

Abstract

This paper presents a comparison of common and well-documented methods for varying the single-diode model parameters extracted at standard test conditions (STC) of a PV module to suit varying operating conditions of irradiance and temperature. To perform such a comparison, accurate values of the single-diode parameters at STC are required. These were obtained using well-established numerical and iterative methods. The Newton-Raphson method was found to be most accurate for obtaining these parameters at STC. Consequently, these parameters were used to compare the methods of varying the single-diode model parameters with temperature and irradiance. MATLAB software has been developed to evaluate the performance of each method using the Shell SQ150 PV module. Results are compared with measured data and discussion of the accuracy of various methods is presented.

© 2017 The Authors. Published by Elsevier Ltd.
Peer-review under responsibility of KES International.

Keywords: PV modelling; Single-diode model; Irradiance; Temperature

1. Introduction

A PV module is commonly modelled using the single-diode model (SDM) of Fig. 1, which also includes the I-V and P-V characteristics of a typical module [1]. The equation representing this model is transcendental and implicit in nature and its solution normally involves considerable computational complexity and may require significant amount of simplifications and approximations [2, 3]. The problem of modelling a PV system is further compounded by the fact that the I-V characteristic of a PV module is dependent on insolation and temperature, which are continuously changing [2, 3, 4]. A Datasheet of a PV module normally provides module's specifications only at standard test conditions (STC). Consequently, the extraction of parameters required to model a PV module/array are extracted at STC and subsequently, these parameters must be adjusted according to the prevailing temperature and

irradiance. The objective of this paper is to provide a comparison between various methods reported in the literature for modifying the single-diode parameters of a PV module to cater for varying conditions of insolation and temperature [3, 5]. Following this introduction, Section 2 presents the mathematical background to the work, whilst Section 3 presents the most commonly known methods of adjusting the parameters of the SDM so as to take into account the effects of insolation and temperature. Section 4 discusses the results obtained during the comparison of these methods and Section 5 outlines the conclusions of the paper.

Nomenclature

E_g	band gap energy of semiconductors (J)
G, G_{STC}	solar irradiance (W/m ²) and irradiance at standard test conditions (STC) (1000 W/m ²).
I	output current of a PV module (A).
I_m, I_{mSTC}	PV module current at the maximum power point (MPP) and at standard test conditions (A).
I_{ph}	photocurrent (A).
I_{sat}, I_{satSTC}	PV module saturation current and its value at standard test conditions (A).
$I_{sc}, I_{sc,STC}$	short-circuit current of a PV module and its value at standard test conditions (A).
k	Boltzmann constant (1.381×10^{-23} J/K).
n	diode ideality factor.
N_s	number of the series-connected cells in a PV module.
P	output power of a PV module (W).
q	electronic charge (-1.602×10^{-19} C).
R_s, R_{sh}	series and shunt resistances of the PV module (Ω)
T, T_{STC}	temperature of the PV module (K) and its temperature at STC (25°C or 298.15 K).
V	output voltage of a PV module (V).
$V_m, V_{m,STC}$	voltage of a PV module at the MPP and its voltage under STC (V).
$V_{oc}, V_{oc,STC}$	open-circuit voltage of a PV module and its voltage at standard test conditions (V).
V_{th}	thermal equivalent voltage of a PV module (V).
$\mu_{V_{oc}}, \mu_{I_{sc}}$	thermal coefficient of the open-circuit voltage (V/°C) and short-circuit current (A/°C).
$\alpha, \beta, \gamma, \text{ and } \delta$	Constants.

2. Mathematical background

Due to its simplicity, the single-diode model, Fig. 1, has been widely used for modelling a PV module [1]. The module terminal current I and voltage V are related by the implicit transcendental equation

$$I = I_{ph} - I_{sat} \left[\exp \left(\frac{V + IR_s}{nN_sV_{th}} \right) - 1 \right] - \frac{V + IR_s}{R_{sh}}, \quad \text{where } V_{th} = \frac{kT}{q} = 25.7 \text{ mV at } 25^\circ\text{C} \quad (1)$$

Clearly, there are five unknown parameters to be determined; the photocurrent source I_{ph} , the ideality factor n , the saturation current I_{sat} , and the series and shunt resistances R_s and R_{sh} respectively of a PV module. Manufacturers' datasheets normally only include data at the remarkable points, namely the short-circuit current I_{sc} , open-circuit voltage V_{oc} , and the maximum power point (MPP) current I_m and voltage V_m . The temperature coefficients of the short-circuit current $\mu_{I_{sc}}$ and of the open-circuit voltage $\mu_{V_{oc}}$ are also provided in addition to the number of series-connected cells in a PV module N_s [2, 3, 4, 5]. To determine the five parameters of a PV module from its datasheet, five equations are required. The remarkable points can be used to generate the following three equations

$$\text{OC: } (V_{oc}, 0): 0 = I_{ph} - I_{sat} \left[\exp\left(\frac{V_{oc}}{n N_s V_{th}}\right) - 1 \right] - \frac{V_{oc}}{R_{sh}} \quad (2)$$

$$\text{SC: } (0, I_{sc}): I_{sc} = I_{ph} - I_{sat} \left[\exp\left(\frac{I_{sc} R_s}{n N_s V_{th}}\right) - 1 \right] - \frac{I_{sc} R_s}{R_{sh}} \quad (3)$$

$$\text{MPP: } I_m = I_{ph} - I_{sat} \left[\exp\left(\frac{V_m + I_m R_s}{n N_s V_T}\right) - 1 \right] - \frac{V_m + I_m R_s}{R_{sh}} \quad (4)$$

In addition, the derivative $dP/dV = 0$ at the MPP is used to develop a fourth equation

$$\left. \frac{dP}{dV} \right|_{MPP} = -\frac{I_m}{V_m} = \frac{-\frac{1}{R_{sh}} - \frac{I_{sat}}{n N_s V_{th}} \exp\left(\frac{V_m + I_m R_s}{n N_s V_T}\right)}{1 + \frac{R_s}{R_{sh}} + \frac{I_{sat} R_s}{n N_s V_{th}} \exp\left(\frac{V_m + I_m R_s}{n N_s V_T}\right)} \quad (5)$$

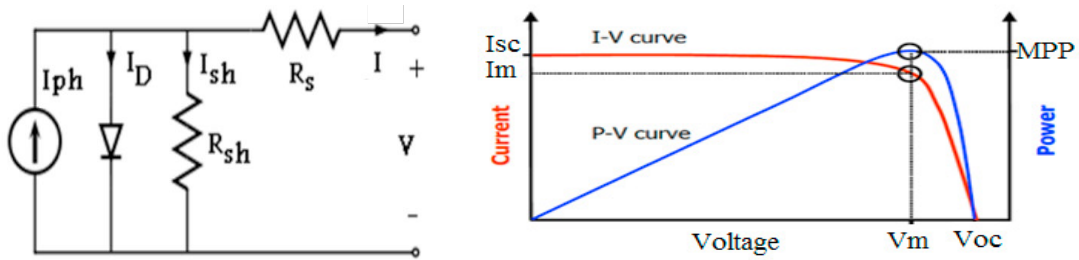


Fig. 1. The single-diode model and typical I-V and PV characteristics of a PV module.

Finally, the reciprocal of the slope of the I-V curve at the short-circuit point, is used to develop the fifth equation needed for parameter extraction of the model [4, 6]:

$$\left. \frac{dI}{dV} \right|_{I_{sc}} = -\frac{1}{R_{sho}} = \frac{-\frac{1}{R_{sh}} - \frac{I_{sat}}{n N_s V_T} \exp\left(\frac{I_{sc} R_s}{n N_s V_T}\right)}{1 + \frac{R_s}{R_{sh}} + \frac{I_{sat} R_s}{n N_s V_T} \exp\left(\frac{I_{sc} R_s}{n N_s V_T}\right)} = -\frac{1}{R_{sh}} \quad (6)$$

Solution of the system of equations (2)-(6) can be obtained numerically, e.g. using Newton-Raphson method, or by applying an iterative method, such as the Gaussian iterative method. Another approach to find the parameters of the single-diode model, which also requires the manufacturer's datasheet and an iterative process hinges on adjusting one of the obtained parameters, such that the value of current or voltage, matching a specific known condition [4, 7, 8, 9, 10]. In [7] the value of the maximum power is used to extract the parameters by setting a value for the ideality factor according to the type of the PV module, and changing the series resistance in an iterative process to calculate the corresponding value of the shunt resistance that produces the same value of the maximum power within a small tolerance. Another relationship between the ideality factor, resistances, and the manufacturer's datasheet at the maximum power point has been derived by restricting the value of the ideality factor, within a small interval, allowing the series and shunt resistances to be estimated [8].

3. Modifying model parameters for varying temperature and insolation

When the performance of PV system is evaluated under certain operating conditions, such as the STC, the practical and theoretical results concur only if the modelling process uses PV parameters which have been extracted under the same operating conditions. Since datasheets only specify a PV module parameters at STC and since these parameters vary considerably with environmental conditions, such as insolation and temperature, adjustments have to be made to the PV module parameters to allow for varying operating conditions. The problem is further complicated by the variations in module parameters with partial shading [11, 12]. However, this paper only focuses on the variations of module parameters with irradiance and temperature, and reviews various methods for catering with such variations for each parameter as presented below.

3.1. The Short-circuit current

There are two common methods to express variations of the short-circuit current I_{sc} with irradiance and temperature.

Method 1: In this method, the short-circuit current is expressed in terms, of G and T, using the following linear empirical relation [1, 7, 13]

$$I_{sc}(G, T) = \frac{G}{G_{STC}} [I_{sc,STC} + \mu_{I_{sc}}(T - T_{STC})] \quad (7)$$

Method 2: The empirical equation (7) results in some deviation in the short-circuit current from experimental results due to the non-linear effect of the solar irradiance. This non-linearity is corrected by the introduction of the exponent α [14, 15, 16] as

$$I_{sc}(G, T) = (G / G_{STC})^\alpha [I_{sc,STC} + \mu_{I_{sc}}(T - T_{STC})], \quad \text{where: } \alpha = \ln(I_{sc,STC} / I_{sc}) / \ln(G_{STC} / G) \quad (8)$$

3.2. Open-circuit voltage

The open-circuit voltage V_{oc} exhibits a strong dependence on temperature, which is described by the voltage temperature coefficient. Its dependence on insolation G is, however, not very significant and follows a logarithmic function. Five common different methods of expressing V_{oc} as a function of T and G have been reported as explained below.

Method 1: In this method, the dependence on insolation is neglected [7, 17], thus

$$V_{oc}(T) = V_{oc,STC} + \mu_{V_{oc}}(T - T_{STC}) \quad (9)$$

Method 2: In this method the dependence of V_{oc} on the insolation is derived from (2) yielding

$$V_{oc}(G) = \ln \left(\frac{I_{ph}(G)R_{sh} - V_{oc}(G)}{I_{sat}R_{sh}} \right) n N_s V_{th} \quad (10)$$

Equation (10) can be solved numerically e.g. using the Newton-Raphson method. The dependence on temperature can be obtained by using (9) [4, 10, 18].

Method 3: Dependence of V_{oc} on insolation and temperature can be derived from (2) [4, 10, 18] giving

$$V_{oc}(G, T) = V_{oc,STC} + \frac{N_s k T n}{q} \ln(G) + \mu_{V_{oc}}(T - T_{STC}) \quad (11)$$

Method4 [1, 5]: This method derived an interpolating relationship between the V_{oc} and G and T as

$$V_{oc}(G, T) = V_{oc,STC} + C_1 \ln(G / G_{STC}) + C_2 \ln(G / G_{STC})^2 + C_3 \ln(G / G_{STC})^3 + \mu_{V_{oc}} (T - T_{STC}) \quad (12)$$

Where $C_1 = 5.468511 \times 10^{-2}$, $C_2 = 5.973869 \times 10^{-3}$, and $C_3 = 7.616178 \times 10^{-4}$ for silicon.

Method 5: This method uses three equations to describe the non-linear effect of G and T on V_{oc} [13, 14, 15] as

$$V_{oc}(G, T) = \frac{V_{oc,STC}}{1 + \beta \ln\left(\frac{G_{STC}}{G}\right)} \left(\frac{T_{STC}}{T}\right)^\gamma, \text{ where } \beta = \frac{(V_{oc,STC} / V_{oc,G}) - 1}{\ln(G_{STC} / G)}, \gamma = \frac{\ln(V_{oc,STC} / V_{oc,T})}{\ln(T / T_{STC})} \quad (13)$$

3.3. The photocurrent current

The photocurrent I_{ph} can be expressed using different model parameters and the datasheet information, therefore, there are different expressions for estimating this current as illustrated below.

Method 1: The saturation current I_{sat} and the series resistance R_s are neglected in (3), hence $I_{ph} = I_{sc}$ [1, 5, 10, 17].

Method 2: When the effect of the resistances is taken into account in (3), the photocurrent becomes [7, 19]

$$I_{ph} = (1 + R_s / R_{sh}) / I_{sc} \quad (14)$$

The same procedure for changing I_{sc} (Method 1) with operating conditions is applied in the above two methods.

Method 3: Using (2) and (3), the photocurrent can be written as [3, 6]

$$I_{ph} = I_{sat} \exp\left(\frac{V_{oc}}{nN_s V_{th}}\right) + \frac{V_{oc}}{R_{sh}} \quad (15)$$

This is based on the assumption that V_{oc} and I_{sat} depend only on temperature. Therefore,

$$I_{ph}(T) = I_{sat}(T) \exp[(V_{oc,STC} + \mu_{V_{oc}}(T - T_{STC})) / nN_s V_{th}(T)] + (V_{oc,STC} + \mu_{V_{oc}}(T - T_{STC})) / R_{sh} \quad (16)$$

The combined effect of G and T can be written as

$$I_{ph}(G, T) = (G / G_{STC}) I_{ph}(T) \quad (17)$$

Method 4 [4]: Combining (2) and (3) without neglecting any terms, the value of the photocurrent can be written as

$$I_{ph,STC} = \left(1 + \frac{R_s}{R_{sh}}\right) I_{sc,STC} \left[\exp\left(\frac{V_{oc,STC}}{nN_s V_{th}}\right) - 1 \right] + \frac{V_{oc,STC}}{R_{sh}} \left[1 - \exp\left(\frac{I_{sc,STC} R_s}{nN_s V_{th}}\right) \right] / \left(\exp\left(\frac{V_{oc,STC}}{nN_s V_{th}}\right) - \exp\left(\frac{I_{sc,STC} R_s}{nN_s V_{th}}\right) \right) \quad (18)$$

The same procedure for changing I_{sc} with operating conditions is applied also in this method.

3.4. Dark saturation current I_{sat}

Most reported works indicate strong dependence of the saturation current I_{sat} on temperature [3, 6], others indicate that it also increases with insolation [20]. In any case, the significant effect of this current on the shape of

the I-V curve near the maximum power, led to five common methods of describing its variations with T and G as presented below.

Method 1: From (2) and (3) with information from the datasheet (i.e. I_{sc} and V_{oc}), variations of the saturation current with temperature can be expressed as [3, 6]

$$I_{sat}(T) = I_{sc,STC} + \mu_{I_{sc}}(T - T_{STC}) - \frac{(V_{oc,STC} + \mu_{V_{oc}}(T - T_{STC}) - (I_{sc,STC} + \mu_{I_{sc}}(T - T_{STC}))R_s) / R_{sh}}{\exp\left(\frac{V_{oc,STC} + \mu_{V_{oc}}(T - T_{STC})}{n N_s V_{th}(T)}\right)} \quad (19)$$

Method 2: This method assumes that $R_{sh} \approx \infty$, and $I_{ph} = I_{sc}$, then from (2) [7, 9, 20]

$$I_{sat} = I_{sc,STC} + \mu_{I_{sc}}(T - T_{STC}) / \left(\exp\left(\frac{V_{oc,STC} + \mu_{V_{oc}}(T - T_{STC})}{n N_s V_{th}}\right) - 1 \right) \quad (20)$$

Method 3: The saturation current is related to the bandgap of semiconductor and temperature by [16, 21, 22, 23]

$$I_{sat}(T) = I_{sat,STC} \left(\frac{T}{T_{STC}} \right)^3 \exp\left[\frac{qE_g}{nk} \left(\frac{1}{T_{STC}} - \frac{1}{T} \right) \right] \quad (21)$$

Method 4: Using (2) and (3), the saturation current can be written as [4]

$$I_{sat} = \frac{(1 + R_s / R_{sh})(I_{sc,STC} + \mu_{I_{sc}}(T - T_{STC})) - (V_{oc,STC} + \mu_{V_{oc}}(T - T_{STC}) + n N_s V_{th} \ln(G)) / R_{sh}}{\exp\left(\frac{V_{oc,STC} + \mu_{V_{oc}}(T - T_{STC}) + n N_s V_{th} \ln(G)}{n N_s V_T}\right) - \exp\left(\frac{(I_{sc,STC} + \mu_{I_{sc}}(T - T_{STC}))R_s}{n N_s V_T}\right)} \quad (22)$$

Method 5: In this method $R_{sh} = \infty$ and $I_{ph,STC} = I_{sc,STC}$ and I_{sat} is obtained from the open-circuit voltage at STC [2, 10]

$$I_{sat}(G, T) = \frac{(G / G_{STC})(I_{sc,STC} + \mu_{I_{sc}}(T - T_{STC})) \exp(q|\mu_{V_{oc}}|(T - T_{STC}) / N_s k n T)}{(G I_{sc,STC} / I_{sat,STC} + 1)^{T_{STC}/T} - \exp(q|\mu_{V_{oc}}|(T - T_{STC}) / N_s k n T)} \quad (23)$$

3.5. Series and shunt resistances R_s and R_{sh}

There are four main methods which describe the effect of the irradiance and temperature on the resistances as presented below.

Method 1: The effect of irradiance and temperature on the resistances is ignored [4, 6, 7, 8, 10]. That is $R_s(G, T) = R_{s,STC}$ and for the shunt resistance $R_{sh}(G, T) = R_{sh,STC}$.

Method 2: The series resistance is assumed constant, i.e. $R_s(G, T) = R_{s,STC}$, while the shunt resistance varies only with the solar irradiance as [17, 20] as

$$R_{sh}(G) = (G_{STC} / G) R_{sh,STC} \quad (24)$$

Method 3: Both resistances vary only with the irradiance [1, 5, 24] i.e. the $R_{sh}(G)$ is given by (24) and

$$R_s = (G_{STC} / G) R_{s,STC} \quad (25)$$

Method 4: In this method, the series resistance increases with temperature and decrease with insolation, while the shunt resistance changes only with insolation according to (24) [21]

$$R_s(G, T) = \frac{T}{T_{STC}} \left(1 - \lambda \ln \frac{G}{G_{STC}} \right) R_{s,STC}, \text{ where } \lambda = 0.217 \quad (26)$$

4. Results and discussion

To evaluate and compare the performance of the above methods in catering for the variations of parameters, with T and G , of a PV module, MATLAB software has been developed to extract parameters of the monocrystalline, Shell SQ150 PV module [26]. Using (8), (13), and the datasheet information, the values of the constants can be obtained as, $\alpha = 0.998$, $\beta = 0.055$, and $\gamma = 1.0797$. In this work, three different methods were used to estimate the single-diode model parameters. The first method uses a preset value for the ideality factor and consequently uses it to calculate the other parameters [7]. The second method uses three boundary conditions to calculate the ideality factor to produce values of the model resistances [8]. The third method uses Newton-Raphson method in which the initial values are calculated according to [27]. As can be seen from Table 1, different methods produced different values of the single-diode model parameters. Fig. 2 shows good agreement between the measured and numerically obtained I-V characteristics of the Shell SQ 150. Therefore, the parameters extracted using the Newton-Raphson method were be used as the reference for the comparison of various methods of adjusting the single-diode model parameters for varying insolation and temperature.

Table1. Shell SQ150 parameters estimation using different methods.			
Parameter	Villalva [7]	Carrero [8]	Newton-Raphson [26]
N	1.3	1.40964	1.4397
R_s (Ω)	0.684	0.61235	0.5906
R_{sh} (Ω)	529.63895	933.77264	1166.1
I_{sat} (A)	7.02317×10^{-8}	2.83113×10^{-7}	4.0163×10^{-7}
I_{ph} (A)	4.80625	4.80315	4.8024

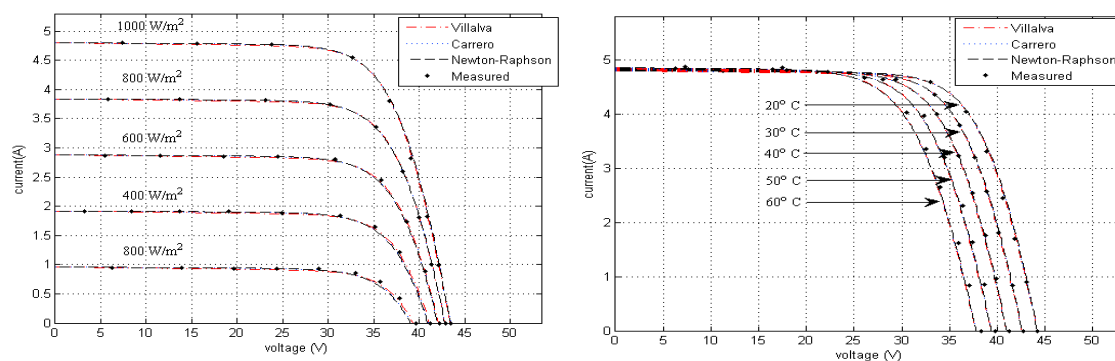


Fig. 2 Comparison between calculated and measured I-V characteristics of the Shell SQ 150 module for three different parameters estimation methods under different irradiance and temperature = 25°C (left) and under different temperature and constant irradiance of 1000 W/m² (right).

Table 2, shows that method 2 has good accuracy compared to method 1, especially for higher values of irradiance. This is because method 2, takes into account the nonlinear effect of irradiance on the current. In general, the absolute error between these methods is relatively small provided that the correct value of α is used.

Table 3 shows the values of the photocurrent for Shell SQ150 module, and these values are compared with the values of the photocurrent obtained from (3). It can be seen that the values of the photocurrent obtained using methods 2 to 4 are close; in particular, method 4 without any approximations gives the same results as (3).

Although, many studies [1, 5, 10, 18] assumed that the photocurrent is equal to the short-circuit current, this assumption can lead to considerable error. The temperature has little effect on the short-circuit current and photocurrent. Table 4 compares the values of the open-circuit voltage at different insulations and it is evident that method 5 has better accuracy. Methods 2 and 3 produced similar results because both methods are based on similar assumptions. Methods 1 and 4 show that ignoring dependence of the open-circuit voltage on irradiance or approximating this effect leads to considerable error. Table 5 shows the relationship between the open-circuit voltage and temperature, indicating that method 2 has better accuracy than Method 1 which can be attributed to the use of accurate value of γ .

Fig. 3 presents a comparison between the methods used to estimate the saturation current under varying irradiance and temperature. It can be seen that simulation results are closer to the experimental results for all five methods, and method 4 is most accurate when compared with other methods because it takes into account the effect of the irradiance on the open-circuit voltage. Fig. 3 also shows a comparison between these methods under varying temperature. It can be seen that the simulation results are closer to the measured data because the improved accuracy of the parameters estimation methods. When the temperature increases, one of the plots tends to deviate from the other methods 1,2,4,5. It can be seen that method 3 provides better accuracy at higher temperatures.

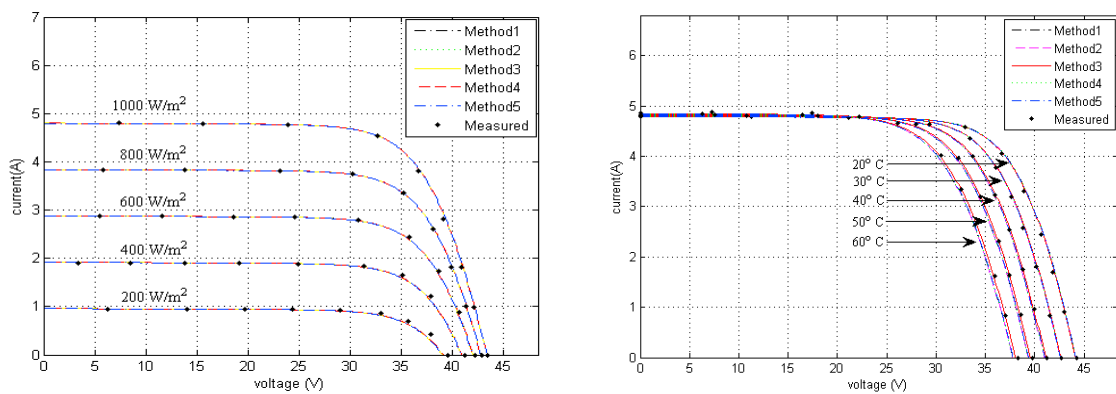


Fig. 3 Comparison between calculated and measured I-V characteristics for different methods of estimating saturation current of the Shell SQ150 module under different irradiance (left) and under different temperature (right).

Fig. 4 shows the effect of the variation in irradiance on the resistances of the module. Methods 1, 2, and 4 give results close to the measured data. The best method that represents the I-V characteristics of the PV module is method 2, which indicates that the shunt resistance decreases with increasing irradiance, while results of Method 4 which are relatively close to those of method 2 show that the series resistance is logarithmically related to irradiance. To verify the changes in the series resistance due to temperature on the I-V characteristics and other parameters, equation (22) was used for this purpose. The figure shows that the variation of the series resistance with temperature, predicted by (22), leads to a deviation of the I-V characteristic from the measured data. This means that variation of the saturation current with temperature is sufficient to represent the behaviour of the PV module alleviating the need to take the effect of the temperature on the series resistance.

Table 2. Methods of changing the short circuit of Shell SQ150 current and the absolute error.

Irradiance(W/m ²)	1000	800	600	400	200
Measured current(A)	4.8	3.8415	2.8817	1.9288	0.94884
Method 1(A) (% error)	4.8 (0%)	3.84 (0.039%)	2.88 (0.059%)	1.92 (0.456%)	0.96 (1.1762%)
Method 2(A) (% error)	4.8 (0%)	3.8417 (0.0052%)	2.8829 (0.042%)	1.9235 (0.275%)	0.9631 (1.5029%)

Table 3. Different values of the photocurrent in the literature

PV module	Generalized Eq.(3)	Method1	Method 2	Method 3	Method 4
Shell SQ150	4.8024316A	4.8 A	4.80243089 A	4.80243114 A	4.80243165 A

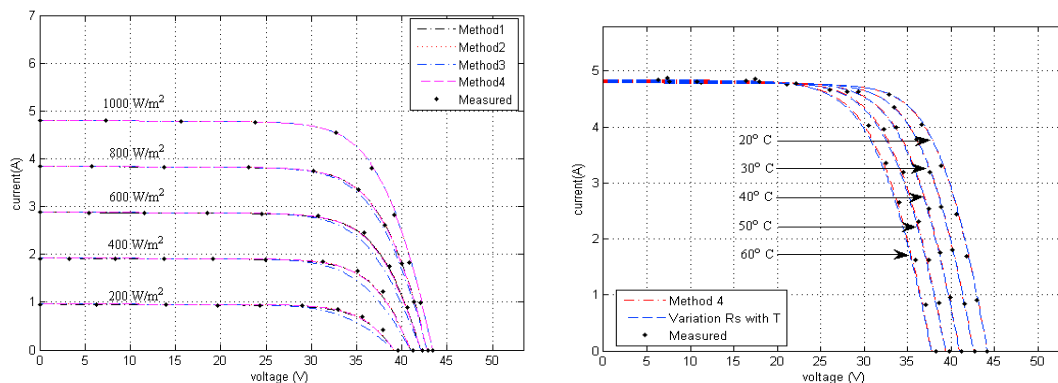


Fig. 4 I-V Comparison between calculated and measured I-V characteristics for different methods of estimating the resistances of the Shell SQ150 module under different irradiance (left) and under different temperature using (22) for changing the saturation current (right).

Table 4. The open-circuit voltage of Shell SQ 150 at different irradiance and absolute error.

Irradiance W/m ²	Measured Voltage (V)	Method 1 (V)	Method 2 (V)	Method 3(V)	Method 4(V)	Method 5(V)
1000	43.4	43.4 0%	43.4 0%	43.4 0%	43.4 0%	43.4 0%
800	42.91547	43.4 1.1165%	42.823523 0.2143%	42.80548 0.2563%	43.38809 1.1013%	42.87381 0.0971%
600	42.22329	43.4 2.7869%	42.05706 0.3937%	42.03902 0.4364%	43.37352 2.7242%	42.21398 0.0221%
400	41.25423	43.4 5.2013%	40.97679 0.6725%	40.95875 0.7164%	43.35267 5.0866%	41.31775 0.15397%
200	39.59298	43.4 8.7719%	39.13005 1.1692%	39.11201 1.2148%	43.32139 9.4169%	39.87068 0.70139%

Table 5. The open-circuit voltage of the Shell SQ 150 at different temperatures and absolute error.

Temperature °C	25	20	30	40	50	60
Measured Voltage(V)	43.4	44.205	42.7315	41.258	39.7845	38.311
Method 1(V)	43.4	44.205	43.3195	40.985	39.375	37.765
% error	0%	0%	1.376%	0.6617%	1.0218%	1.4252%
Method 2(V)	43.4	44.2002	42.6273	41.1587	39.7846	38.4962
% error	0%	0.0109%	0.2439%	0.2407%	0.00025%	0.4834%

5. Conclusion

The paper presented various methods for adjusting the model parameters of the single-diode model according to varying levels of irradiance and temperature. The relative accuracy of these methods was assessed by comparing the values of the adjusted parameters with measured data available in the datasheet. The short-circuit current varies nonlinearly with irradiance and its variation with temperature is fairly small depending on its temperature coefficient. Prediction of the photocurrent by various methods, showed that its variations with temperature and irradiance are similar to those of the short-circuit current. When determining the dependence of the open-circuit voltage on temperature and irradiance, it is found that Method 5 gives good results because it involves less

approximations and takes into account effects of both temperature and irradiance simultaneously. The accuracy in determining the open-circuit voltage is improved by taking into account the nonlinear effects of both temperature and irradiance. In predicting the saturation current, method 4 is most accurate when considering the effect of varying temperature and irradiance. Changes of the shunt resistance with irradiance are much higher than those exhibited by the series resistance. Both resistances have little sensitivity to changes in temperature.

References

- [1] Brano V L, Orioli A, Ciulla G, Gangi A D. An improved five-parameter model for photovoltaic modules. . Solar Energy Materials and Solar Cells 2010; 94(8): 1358-1370.
- [2] Mahmoud Y, Xiao W, Zeineldin H H. A Simple Approach to Modeling and Simulation of Photovoltaic Modules. IEEE Transactions on Sustainable Energy 2011; 3(1): 185-186.
- [3] Chatterjee A, Keyhani A, Kapoor D. Identification of Photovoltaic Source Models. IEEE Transactions on Energy Conversion 2011; 26(3): 883-889.
- [4] Siddique H, Xu P, De Doncker R. Parameter extraction algorithm for one-diode model of PV panels based on datasheet values. 2013 International Conference on Clean Electrical Power (ICCEP). 2013.
- [5] Orioli A, Gangi A D. A procedure to calculate the five-parameter model of crystalline silicon photovoltaic modules on the basis of the tabular performance data. Applied Energy 2013; 102(1): 1160–1177.
- [6] Sera D, Teodorescu R, Rodriguez P. Photovoltaic module diagnostics by series resistance monitoring and temperature and rated power estimation. 2008 34th Annual Conference of IEEE Industrial Electronics. 2008.
- [7] Villalva MG, Gazoli JR, Filho ER. Comprehensive approach to modeling and simulation of photovoltaic arrays. IEEE Trans. Power Electron 2009; 94(5): 1198-1208.
- [8] Carrero C, Ramírez D, Rodríguez J, Platero C. Accurate and fast convergence method for parameter estimation of PV generators based on three main points of the I–V curve. Renewable Energy 2011; 36(11): 2972-2977.
- [9] 3. Can H, Ickilli D, Parlak K. A New Numerical Solution Approach for the Real-Time Modeling of Photovoltaic Panels. 2012 Asia-Pacific Power and Energy Engineering Conference. 2012.
- [10] Mahmoud Y A, Xiao W, Zeineldin H H. A Parameterization Approach for Enhancing PV Model Accuracy. IEEE Transactions on Industrial Electronics 2013; 60(12): 5708-5716.
- [11] Anani N, Shahid M, Al-kharji O, Ponciano J. A CAD Package for Modeling and Simulation of PV Arrays. Elsevier Energy Procedia 2013; 42(1): 397-405.
- [12] 4. Burns P, Anani N. Modelling and simulation of photovoltaic arrays under varying conditions. 2014 9th International Symposium on Communication Systems, Networks & Digital Sign (CSNDSP). 2014.
- [13] Cubas J, Pindado S, Victoria M. On the analytical approach for modeling photovoltaic systems behavior. Journal of Power Sources 2014; 247(1): 467-474.
- [14] Khezzar R, Zereg M, Khezza A. Modeling improvement of the four parameter model for photovoltaic modules. 2014; 110(1): 452-462.
- [15] Zhou W, Yang H, Fang Z. A novel model for photovoltaic array performance prediction. Applied Energy 2007; 84(12): 1187-1198.
- [16] Dongue S B, Njomo D, Ebengai L. An Improved Nonlinear Five-Point Model for Photovoltaic Modules. International Journal of Photoenergy, article ID 680213. 2013.
- [17] Soto W, Klein S, Beckman W. Improvement and validation of a model for photovoltaic array performance. Solar Energy 2006; 80(1): 78-88.
- [18] Bellini A, Bifaretti S, Iacovone V, Cornaro C. Simplified model of a photovoltaic module. Proc. Applied Electronics Conference, 2009.
- [19] Ghani F, Duke M. Numerical determination of parasitic resistances of a solar cell using the Lambert W-function. Solar Energy 2011; 85(9): 2386-2394.
- [20] Chegaar M, Hamzaoui A, Namoda A, Petit P, Aillerie M, Herguth A. Effect of Illumination Intensity on Solar Cells Parameters. Energy Procedia 2013; 36: 722-729.
- [21] Islam M, Djokic S, Desmet J, Verhelst B. Measurement based modelling and validation of PV systems. Proc. IEEE Power Tech, Grenoble, 2013.
- [22] Bai J, Liu S, Hao Y, Zhang Z, Jiang M, Zhang Y. Development of a new compound method to extract the five parameters of PV modules. Energy Conversion and Management 2014; 79, 294-303.
- [23] Ghani F, Duke M. Numerical determination of parasitic resistances of a solar cell using the Lambert W-function. Solar Energy 2011; 85(9): 2386-2394.
- [24] Ghani F, Duke M, Carson J. Numerical calculation of series and shunt resistance of a photovoltaic cell using the Lambert W-function: Experimental evaluation. Solar Energy 2013; 87: 246-253.
- [25] Ma J, Man K, Ting T O, Zhang N, Lim E, et al. Simple Computational Method of Predicting Electrical Characteristics in Solar Cells. Elektronika Ir Elektrotechnika 2014; 20(1): 1392-1215.
- [26] SQ150 PV module datasheet. [Internet]. 2017 [cited 24 March 2017]. Available from: <http://www.physics.arizona.edu/~cronin/Solar/TEP%20module%20spec%20sheets/Shell%20SQ150.pdf>
- [27] Can H, Ickilli D. Parameter estimation in modeling of photovoltaic panels based on datasheet values. Solar Energy Engineering 2013; 136(2).